Adsorption of water on graphene: A van der Waals density functional study

Ikutaro Hamada*

Advanced Institute for Materials Research (AIMR), Tohoku University, Sendai 980-8577, Japan

(Received 26 August 2012; published 30 November 2012)

The van der Waals density functional (vdW-DF) was used to investigate the interaction of a water monomer with graphene. It was found that a variant of vdW-DF [Hamada and Otani, Phys. Rev. B **82**, 153412 (2010)] predicts geometries and energetics of water on graphene which are in good agreement with those obtained using more elaborate random-phase approximation and quantum Monte Carlo approaches. Interfacial electronic structures were also analyzed in detail.

DOI: 10.1103/PhysRevB.86.195436 PACS number(s): 61.48.Gh, 68.43.Bc, 71.15.Mb, 73.20.Hb

I. INTRODUCTION

Water at interfaces plays a critical role in diverse disciplines, ranging from daily life to science and technology, including wetting, lubrication, corrosion, heterogeneous catalysis, and electrochemistry, to name but a few. Recent studies highlight the role of water at nanoscale in a rich variety of phenomena, such as heterogeneous ice nucleation,[1] friction,[2,3] and lubrication.[4] Water is known to exhibit anomalous properties when confined in nanostructures, and in particular, water confined in carbon nanostructures has attracted much attention.[5–9] However, the mechanism of anomalous behavior of confined water in carbon nanostructures remains to be explored. This is, in part, because of the difficulty in describing the interaction between water molecules and that between water and walls (surfaces), which are weak in general and still challenging even with a modern density functional theory (DFT) based approach.

In many simulations of bulk as well as confined water, classical force fields have been employed to describe the interatomic interactions. The force fields used are, however, mostly constructed so as to reproduce the properties of bulk or small molecules obtained from experiments or accurate quantum-mechanical calculations, and their accuracy in describing interfaces has yet to be examined. Thus, it is important to describe the interaction between water and (carbon) walls, as well as that between water molecules with similar accuracy, to predict confined water. Furthermore, it was proposed[10] that the fast diffusion of water in confined water is attributed to the subtle electronic rearrangement of water interfacing with the surface, and explicit treatment of electronic structure is essential.

In this work, the interaction between water and graphene has been studied by means of the van der Waals density functional (vdW-DF)[11] and its variants. The vdW-DF is a promising density functional which is able to describe weak van der Waals (vdW) interaction as well as covalent interaction in a seamless fashion. It was also shown that vdW-DF is able to describe hydrogen bonding with reasonable accuracy.[12–16] I show that by choosing the appropriate exchange and nonlocal correlation in vdW-DF, the interaction between water and graphene is described accurately, which is comparable to the results obtained with elaborate and highly accurate approaches, such as random-phase approximation (RPA) and the diffusion Monte Carlo (DMC) method.

II. METHOD

All the calculations were performed using the ultrasoft pseudopotentials[17] and a plane-wave basis set as implemented in the STATE code.[18] Wave functions and augmentation charge density were expanded in terms of a plane-wave basis set with cutoff energies of 25 and 225 Ry, respectively. A (5×5) surface supercell was used, and only the Γ point was used to sample the Brillouin zone. The Perdew-Burke-Ernzerhof (PBE) exchange-correlation functional was used for calculations within the generalized gradient approximation (GGA). The PBE-optimized lattice constant (0.2467 nm) was used to construct the supercell (see also Ref. 19), and the graphene sheets were separated by a 2-nm-thick vacuum. A spurious electrostatic interaction between image graphene layers[20] was eliminated by solving the Poisson equation for the open boundary condition for the surface-normal direction exactly, using the Green's function technique.[21] For the vdW-DF calculations, I used the C09 (Ref. 22) exchange in conjunction with the nonlocal correlation of vdW-DF2 (Ref. 23; vdW-DF2$^{\mathrm{C09}_x}$). vdW-DF2$^{\mathrm{C09}_x}$ is shown to outperform vdW-DF and vdW-DF2 in describing graphene adsorption on metal surfaces:[19] The original vdW-DF is known to overestimate equilibrium adsorption distance and vdW interaction near the equilibrium because of the too repulsive exchange used [revised PBE (revPBE)] and too attractive nonlocal correlation near the equilibrium. The C09 exchange is designed to match the gradient expansion approximation in the slowly varying limit, and the vdW-DF2 nonlocal correlation gives a more accurate vdW attraction than the original one by employing a large-N asymptote in determining the internal function, and thus vdW-DF2$^{\mathrm{C09}_x}$ provides a good description of adsorption systems. For comparison, calculations were performed with vdW-DF, vdW-DF2, and vdW-DFs with PBE, optimized PBE,[24] and optimized Becke[24] exchange functionals, which are denoted by vdW-DF$^{\mathrm{PBE}_x}$, optPBE-vdW, and optB86b-vdW, respectively. The vdW-DF calculations were performed non-self-consistently (NSC) as a post-GGA perturbation, using the self-consistent PBE charge densities.

III. RESULTS AND DISCUSSION

I calculated the interaction energy as a function of distance between the water molecule and graphene sheet for one-leg and two-leg configurations, with PBE and vdW-DFs (Fig. 1).

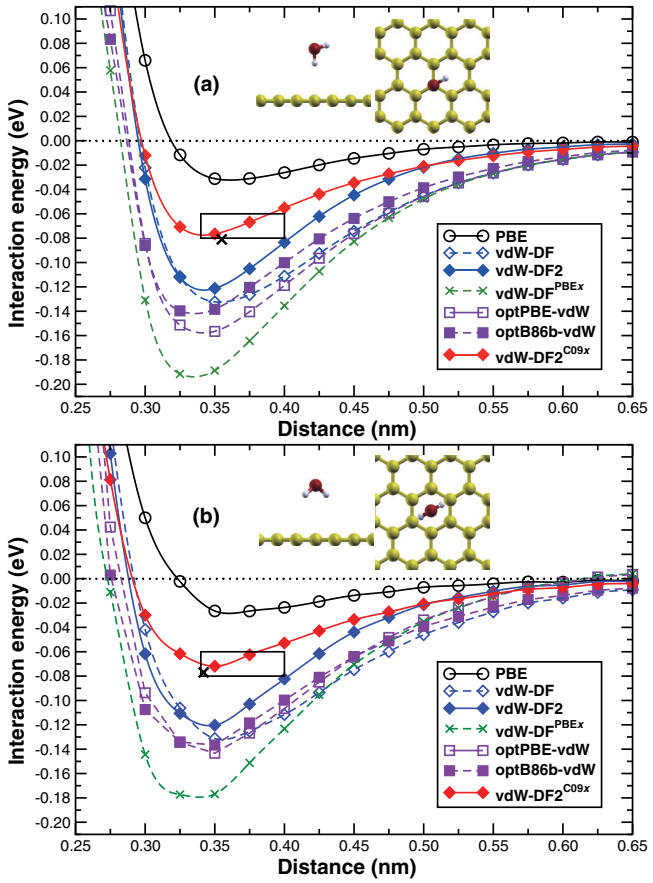

FIG. 1. (Color online) Interaction energy of water with graphene as a function of graphene-water distance for (a) one-leg and (b) two-leg configurations. Lines were obtained by spline fitting. The graphene-water distance is defined as the vertical distance between the graphene sheet and the O atom of the water molecule. Insets show side and top views of water on graphene. The results obtained with the random-phase approximation are shown by the crosses. The quantum Monte Carlo results are within the rectangles, indicating the error bars in the calculations.

Other configurations of water on several adsorption sites were investigated by Kurita *et al.*[25] with GGA. The calculated equilibrium distances and interaction energies are summarized in Table I. The present GGA results are in good agreement with those reported in the literature.[25–27] While GGA predicts a small interaction energy of the water monomer on graphene, vdW-DF predicts a much larger interaction energy, suggesting the importance of the vdW interaction between water and graphene. Notably, the equilibrium distances and interaction energies calculated with vdW-DF2^{C09_x} are in good agreement with those obtained with RPA and DMC. Other vdW-DFs overestimate the interaction energies of the systems, although they predict interaction energies in good agreement with those obtained by using vdW-DF,[28] the density functional/coupled-cluster method,[29] extrapolation of interaction energy between water and acene with DFT-based symmetry-adapted perturbation theory,[30] and the coupled-cluster method.[31] However, the results obtained using explicitly correlated methods[29–31] may be less accurate in describing water adsorbed on graphene because the correlation effects were included locally, and the inherent extended nature of graphene is not taken into account in the calculation of correlation energy. Our results with vdW-DF2^{C09_x} are also in good agreement with those obtained using revPBE with dispersion correction based on the Wannier functions (vdW-WF).[27] Overestimation of the equilibrium distance with vdW-WF based on revPBE is mainly because of the too repulsive revPBE exchange. vdW-WF based on PBE overestimates the interaction energies because of the spurious binding of the PBE exchange. It is noted that vdW-DF with C09 exchange and nolocal correlation of vdW-DF overestimates the interaction energy, as the use of the nonlocal correlation of the original vdW-DF gives a too attractive vdW interaction near the equilibrium. The accuracy of vdW-DF2^{C09_x} in describing water adsorption on graphene suggests that the C09 exchange describes the exchange repulsion in the vicinity of the graphene surface reasonably well.

To confirm the validity of the NSC approach, self-consistent vdW-DF[32] calculations were performed by using the SIESTA[33] code with the efficient implementation by Román-Peréz and Soler.[34] The Troullier-Martins norm-conserving pseudopotentials and triple-zeta plus polarization basis was used. The effect of pseudopotentials used in vdW-DF calculations[35] was examined by performing vdW-DF calculations with pseudopotentials and pseudoatomic orbitals generated using PBE-GGA (vdW-DF2^{C09_x}@PBE) and vdW-DF2^{C09_x}. Other details of the SIESTA calculation can be found in Ref. 36. As shown in Table I, self-consistency and pseudopotential effects on the equilibrium distance and interaction energy are minor ($\lesssim 10^{-3}$ nm and <3 meV, respectively), corroborating the present NSC vdW-DF approach.

In order to gain insights into the adsorption mechanism of water on graphene, I calculated the charge-density difference defined by $\Delta\rho(\mathbf{r}) = \rho_{\rm tot}(\mathbf{r}) - \rho_{\rm gra}(\mathbf{r}) - \rho_{\rm H_2O}(\mathbf{r})$, where $\rho_{\rm tot}(\mathbf{r})$, $\rho_{\rm gra}(\mathbf{r})$, and $\rho_{\rm H_2O}(\mathbf{r})$ are the charge densities of the adsorption system, isolated graphene, and the isolated H_2O molecule, respectively. I also calculated the spatial distribution of the nonlocal binding energy,

$$\Delta e_{\rm c}^{\rm NL}(\mathbf{r}) = e_{\rm c,tot}^{\rm NL}(\mathbf{r}) - e_{\rm c,gra}^{\rm NL}(\mathbf{r}) - e_{\rm c,H_2O}^{\rm NL}(\mathbf{r}), \qquad (1)$$

where $e_{\rm c,tot}^{\rm NL}(\mathbf{r})$, $e_{\rm c,gra}^{\rm NL}(\mathbf{r})$, and $e_{\rm c,H_2O}^{\rm NL}(\mathbf{r})$ are the nonlocal correlation energy densities for the adsorption system, isolated graphene, and the isolated H_2O molecule, respectively, where the nonlocal correlation is defined by

$$E_{\rm c}^{\rm NL} = \frac{1}{2}\iint d\mathbf{r}d\mathbf{r}'\rho(\mathbf{r})\phi(\mathbf{r},\mathbf{r}')\rho(\mathbf{r}') = \int d\mathbf{r}e_{\rm c}^{\rm NL}(\mathbf{r}). \qquad (2)$$

$\phi(\mathbf{r},\mathbf{r}')$ is the vdW kernel, which is a function of ρ and its gradient $|\nabla\rho|$, as given in Ref. 11. $\Delta\rho$ and $\Delta e_{\rm c}^{\rm NL}$ for one-leg and two-leg configurations are shown in Fig. 2. It turns out that graphene is polarized considerably upon adsorption of the water molecule [Figs. 2(a) and 2(b)], and electrostatic interaction plays a role in attractive interaction. The polarization is larger in the one-leg configuration than in the two-leg one, giving a larger interaction energy. This explains the water adsorption and relative stability of the water molecule within GGA. $\Delta e_{\rm c}^{\rm NL}$, which is localized in the vicinity of graphene and the water molecule [Figs. 2(c) and 2(d)], gives the vdW attraction and is larger in magnitude for the one-leg configuration ($\Delta e_{\rm c}^{\rm NL}$ is more localized in the vicinity of a hydrogen atom pointing toward graphene). Thus, both

TABLE I. Equilibrium distances d_0 and interaction energies E_0 for one-leg and two-leg configurations obtained using plane-wave (PW) and pseudoatomic orbital (PAO) basis sets.

	One-leg configuration		Two-leg configuration	
Method	d_0 (nm)	E_0 (eV)	d_0 (nm)	E_0 (eV)
		PW		
PBE	0.3607	−0.032	0.3612	−0.028
vdW-DF	0.3533	−0.133	0.3548	−0.132
vdW-DF2	0.3423	−0.123	0.3432	−0.121
vdW-DF$^{\mathrm{PBE}_x}$	0.3346	−0.195	0.3369	−0.181
optPBE-vdW	0.3400	−0.159	0.3446	−0.144
optB86b-vdW	0.3353	−0.143	0.3398	−0.139
vdW-DF2$^{\mathrm{C09}_x}$	0.3420	−0.078	0.3465	−0.072
		PAO		
PBE	0.3617	−0.0300	0.3704	−0.027
vdW-DF2$^{\mathrm{C09}_x}$@PBE	0.3441	−0.0802	0.3436	−0.073
vdW-DF2$^{\mathrm{C09}_x}$	0.3426	−0.0751	0.3431	−0.071
DMC[a]	0.34–0.40	-0.07 ± 0.01	0.34–0.40	-0.07 ± 0.01
RPA[a]	0.355	−0.081	0.342	−0.077

[a]Reference 26.

the electrostatic and vdW attractions are larger for the one-leg configuration than in the two-leg one, resulting in the larger interaction energy for the former.

In Fig. 3, the band structures for graphene and those with different water orientations are shown.[37] The band structures were calculated using the charge density and potential obtained

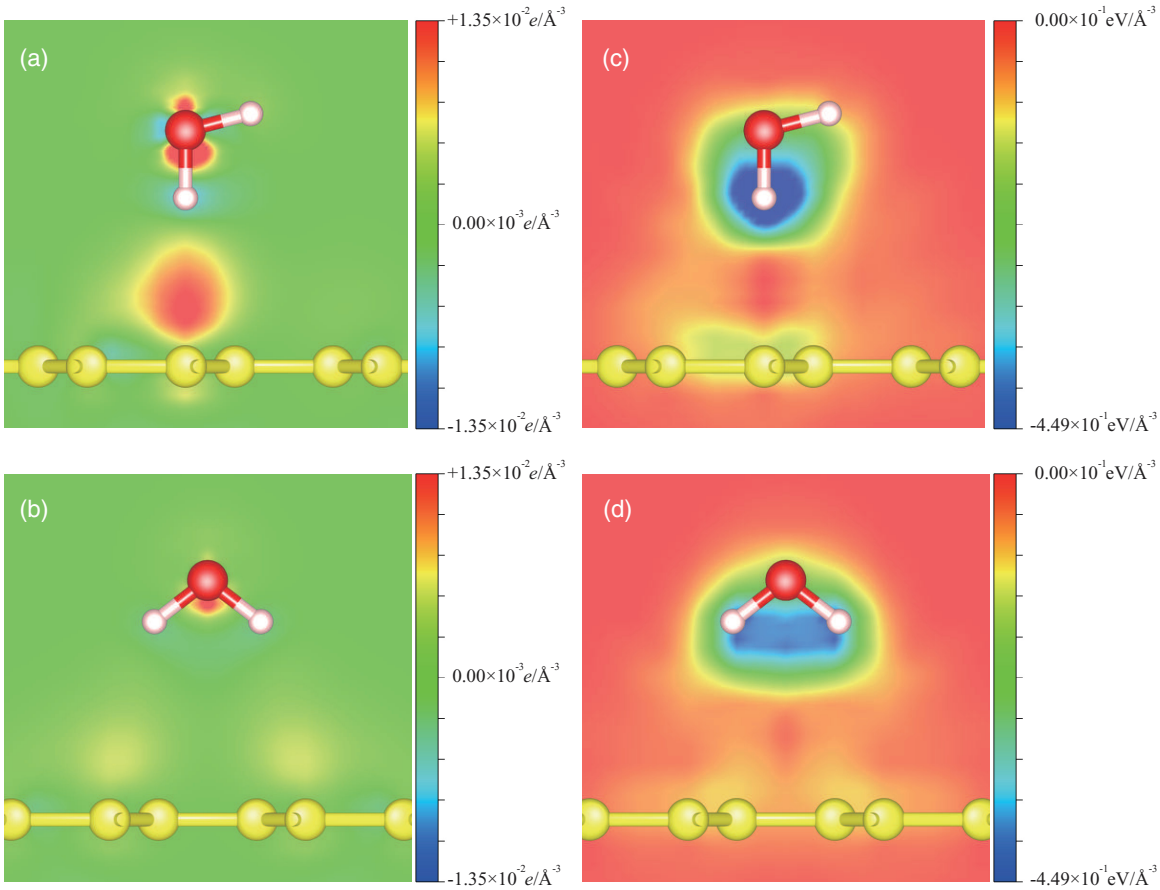

FIG. 2. (Color online) Charge-density difference $\Delta\rho$ and nonlocal binding energy Δe_c^{NL} for one-leg [(a) and (c), respectively] and two-leg [(b) and (d), respectively] configurations.

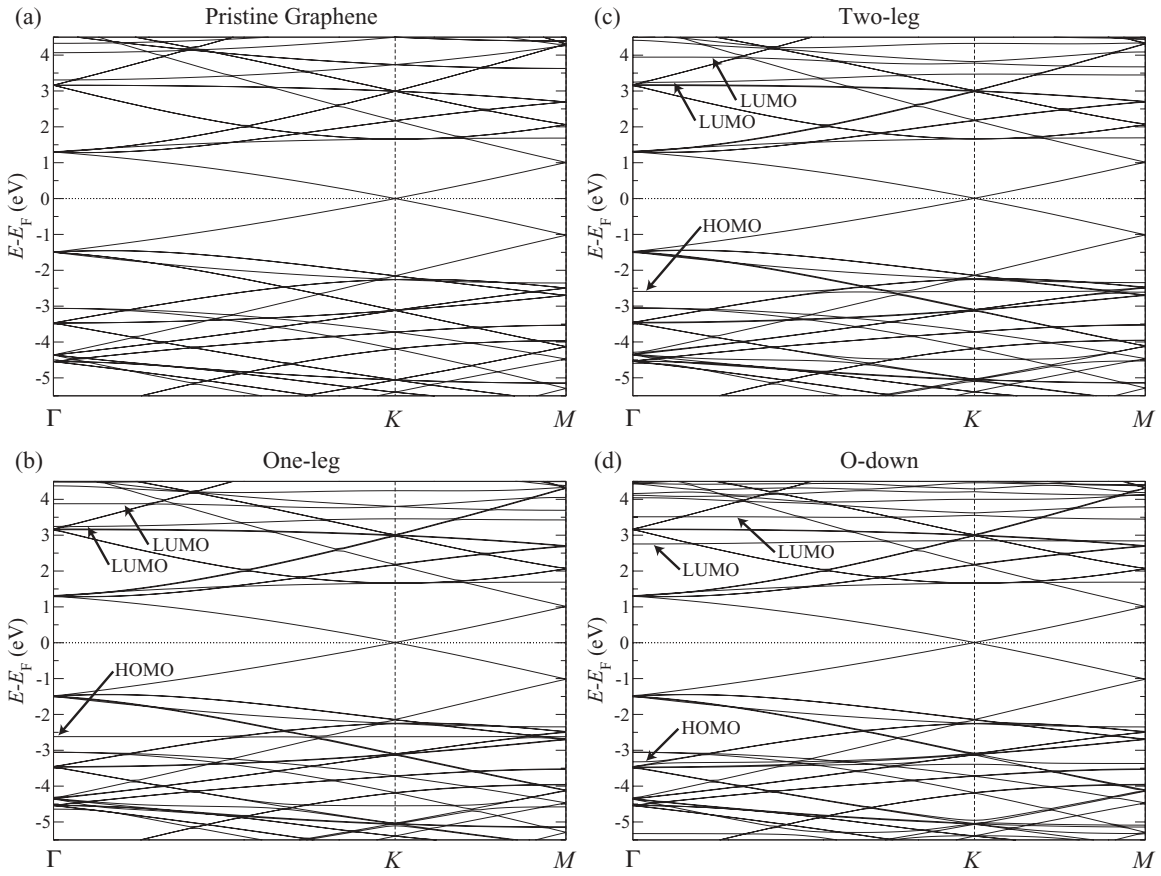

FIG. 3. Band structures of (a) pristine graphene and those of graphene with water in (b) the one-leg, (c) two-leg, and (d) O-down configurations. The states derived from HOMO and LUMO are indicated by the arrows.

with a 12×12 k point to locate the Dirac point at K to the Fermi level E_F accurately. To compare the effect of geometry, the band structure of an O-down configuration, in which the O atom in water points toward graphene, was also calculated.[38] Because the interaction between water and graphene is very weak, the band structures of graphene with water molecules are identical to that of the pristine graphene, except for the tiny splitting of some bands due to the symmetry lowering upon water adsorption and additional energy levels originating from water molecular orbitals. No doping effect was observed, in agreement with Refs. 39, 40, and 41. The highest occupied molecular orbital (HOMO) of the water molecule is located at -2.62, -2.60, and -3.33 eV relative to the Fermi level E_F for the one-leg, two-leg, and O-down configurations, respectively. On the other hand, the lowest unoccupied molecular orbital (LUMO) forms weakly hybridized states with the nearly free electron (NFE) states of pristine graphene, which are discernible at 3.31, 4.07, and 4.33 eV relative to E_F at the Γ point [Fig. 3(a)]. In the case of the one-leg configuration [Fig. 3(b)], LUMO hybridizes with a NFE state, which is apparent from the LUMO-derived states at $E_F + 3.25$ eV and $E_F + 3.89$ eV at the Γ point with dispersion. The wave function corresponding to the former eigenvalue has a slightly larger amplitude in graphene. In the two-leg case [Fig. 3(c)], LUMO forms hybridized states located at 3.26 and 3.96 eV relative to E_F, with the former having a larger amplitude of the graphene wave function. The hybridized states are located at 2.75 and 3.51 eV relative to E_F in the O-down configuration [Fig. 3(d)], and the latter has a larger amplitude of the graphene wave function, which is the opposite of the two-leg case, suggesting the role of the water dipole moment in determining the position of the hybridized states. The HOMO-LUMO gap was estimated from the energy levels of HOMO and the lowest hybridized state derived from LUMO at the Γ point, leading to 5.87, 5.85, and 6.08 eV for the one-leg, two-leg, and O-down configurations, respectively. The HOMO-LUMO gaps for the adsorbed water molecules are slightly smaller than the calculated gas-phase value (6.18 eV) because of the hybridization of molecular orbitals with substrate states and not the image potential effect,[42] which is entirely missing in a conventional semilocal density approximation.

It is noted that there are slight discrepancies with Ref. 41 in the positions of the water molecular levels and those of NFE states when a water molecule is adsorbed. I presume these discrepancies are attributed to the difference in the supercell used, the distance between water and graphene, and, most importantly, the artificial electrostatic interaction (electric field) as a result of the periodic boundary condition in Ref. 41. In the present calculations, however, such artificial interaction is eliminated. Although the differences in energy levels are very small, this fact suggests the importance of accurate treatment of the electrostatic interaction in describing water molecules, which have a considerable dipole moment. In particular, because they are very sensitive to the external

electric field,[43] care must be taken in examining the field effect of the NFE states of graphene.

IV. SUMMARY

The geometry and electronic state of water on graphene have been investigated by means of vdW-DF. It is shown that vdW-DF2^{C09_x} predicts the equilibrium distance and interaction energy in good agreement with those obtained using RPA and DMC. The structures of water confined in nanostructures and on surfaces are determined by the subtle balance between water-surface interaction and hydrogen bonding between water molecules. Thus, new insight into confined and adsorbed water may be obtained with vdW-DF, as it modifies the GGA description of the water-surface interaction. Applications of vdW-DF to water confined in carbon nanostructures are highly anticipated.

ACKNOWLEDGMENTS

I thank Arunabhiram Chutia for a careful reading of the manuscript. This work was partly supported by a Grant-in-Aid for Scientific Research on Innovative Area "Materials Design through Computics: Complex Correlation and Non-equilibrium Dynamics" from the Ministry of Education, Culture, Sports, Science and Technology (MEXT), Japan, under Contract No. 23104501. Advanced Institute for Materials Research was established by the World Premier International Research Center Initiative (WPI), MEXT, Japan. Molecular structures were visualized by the XCRYSDEN[44] and VESTA[45] software packages.

*ikutaro@wpi-aimr.tohoku.ac.jp

[1] A. Michaelides and K. Morgenstern, Nat. Mater. **6**, 597 (2007).
[2] K. B. Jinesh and J. W. M. Frenken, Phys. Rev. Lett. **96**, 166103 (2006).
[3] K. B. Jinesh and J. W. M. Frenken, Phys. Rev. Lett. **101**, 036101 (2008).
[4] K. Falk, F. Sedlmeier, L. Joly, R. R. Netz, and L. Bocquet, Nano Lett. **10**, 4067 (2010).
[5] G. Hummer, J. C. Rasalah, and J. P. Noworyta, Nature (London) **414**, 188 (2001).
[6] K. Koga, G. T. Gao, H. Tanaka, and X. C. Zeng, Nature (London) **412**, 802 (2001).
[7] O. Beckstein and M. S. P. Sansom, Proc. Natl. Acad. Sci. USA **100**, 7063 (2003).
[8] M. Majumder, N. Chopra, R. Andrews, and B. J. Hinds, Nature (London) **438**, 44 (2005).
[9] J. K. Holt, H. G. Park, Y. Wang, M. Stadermann, A. B. Artyukhin, C. P. Grigoropoulos, A. Noy, and O. Bakajin, Science **312**, 1034 (2006).
[10] G. Cicero, J. C. Grossman, E. Schwegler, F. Gygi, and G. Galli, J. Am. Chem. Soc. **130**, 1871 (2008).
[11] M. Dion, H. Rydberg, E. Schröder, D. C. Langreth, and B. I. Lundqvist, Phys. Rev. Lett. **92**, 246401 (2004).
[12] A. K. Kelkkanen, B. I. Lundqvist, and J. K. Nørskov, J. Chem. Phys. **131**, 046102 (2009).
[13] J. Klimeš, D. R. Bowler, and A. Michaelides, J. Phys. Condens. Matter **22**, 022201 (2010).
[14] I. Hamada, K. Lee, and Y. Morikawa, Phys. Rev. B **81**, 115452 (2010).
[15] I. Hamada, J. Chem. Phys. **133**, 214503 (2010).
[16] B. Kolb and T. Thonhauser, Phys. Rev. B **84**, 045116 (2011).
[17] D. Vanderbilt, Phys. Rev. B **41**, 7892 (1990).
[18] Y. Morikawa, H. Ishii, and K. Seki, Phys. Rev. B **69**, 041403(R) (2004).
[19] I. Hamada and M. Otani, Phys. Rev. B **82**, 153412 (2010).
[20] I. Hamada, M. Otani, O. Sugino, and Y. Morikawa, Phys. Rev. B **80**, 165411 (2009).
[21] M. Otani and O. Sugino, Phys. Rev. B **73**, 115407 (2006).
[22] V. R. Cooper, Phys. Rev. B **81**, 161104(R) (2010).
[23] K. Lee, É. D. Murray, L. Kong, B. I. Lundqvist, and D. C. Langreth, Phys. Rev. B **82**, 081101(R) (2010).
[24] J. Klimeš, D. R. Bowler, and A. Michaelides, Phys. Rev. B **83**, 195131 (2011).
[25] T. Kurita, S. Okada, and A. Oshiyama, Phys. Rev. B **75**, 205424 (2007).
[26] J. Ma, A. Michaelides, D. Alfé, L. Schimka, G. Kresse, and E. Wang, Phys. Rev. B **84**, 033402 (2011).
[27] A. Ambrosetti and P. L. Silvestrelli, J. Phys. Chem. C **115**, 3695 (2011).
[28] X. Li, J. Feng, E. Wang, S. Meng, J. Klimeš, and A. Michaelides, Phys. Rev. B **85**, 085425 (2012).
[29] M. Rubeš, P. Nachtigall, J. Vondrášek, and O. Bludský, J. Phys. Chem. C **113**, 8412 (2009).
[30] G. R. Jenness, O. Karalti, and K. D. Jordan, Phys. Chem. Chem. Phys. **12**, 6375 (2010).
[31] E. Voloshina, D. Usvyat, M. Schütz, Y. Dedkov, and B. Baulus, Phys. Chem. Chem. Phys. **13**, 12041 (2011).
[32] T. Thonhauser, V. R. Cooper, S. Li, A. Puzder, P. Hyldgaard, and D. C. Langreth, Phys. Rev. B **76**, 125112 (2007).
[33] J. M. Soler, E. Artacho, J. D. Gale, A. García, J. Junquera, P. Ordejón, and D. Sánchez-Portal, J. Phys. Condens. Matter **14**, 2745 (2002).
[34] G. Román-Pérez and J. M. Soler, Phys. Rev. Lett. **103**, 096102 (2009).
[35] I. Hamada and S. Yanagisawa, Phys. Rev. B **84**, 153104 (2011).
[36] The lattice constant of graphene was optimized using a (1×1) unit cell with a 12×12 k-point set, and the Fermi level was treated using the Mathefessel-Paxton scheme with a smearing width of 25 meV. The equilibrium lattice constant obtained with triple zeta plus polarization (TZP) [double zeta plus polarization (DZP)] is 0.2490 (0.2498) and 0.2488 (0.2496) nm for PBE and vdW-DF, respectively. The equilibrium OH bond length and HOH bond angle with TZP (DZP) are 0.1851 (0.1846) nm and 104.045° (104.593°) for PBE and 0.1852 (0.1849) nm and 104.456° (104.787°) for vdW-DF.
[37] Band structures were calculated at the vdW-DF2^{C09_x} equilibrium distances with PBE. It is noted that in the non-self-consistent vdW-DF, only the total energy is evaluated using the charge density self-consistently determined with PBE, and thus, the Kohn-Sham eigenvalues are evaluated with PBE. However, the band structures

obtained with PBE and self-consistent vdW-DF at the same geometry are shown to be identical.[35]

[38]The calculated equilibrium distance and interaction energy for the O-down configuration are 0.3173 nm and −0.066 eV, respectively.

[39]O. Leenaerts, B. Partoens, and F. M. Peeters, Phys. Rev. B **77**, 125416 (2008).

[40]R. M. Ribeiro, N. M. R. Peres, J. Coutinho, and P. R. Briddon, Phys. Rev. B **78**, 075442 (2008).

[41]T. O. Wehling, A. I. Lichtenstein, and M. I. Katsnelson, Appl. Phys. Lett. **93**, 202110 (2008).

[42]J. B. Neaton, M. S. Hybertsen, and S. G. Louie, Phys. Rev. Lett. **97**, 216405 (2006).

[43]M. Otani and S. Okada, J. Phys. Soc. Jpn. **79**, 073701 (2010).

[44]A. Kokalj, Comput. Mater. Sci. **28**, 155 (2003).

[45]K. Momma and F. Izumi, J. Appl. Crystallogr. **44**, 1272 (2011).